Materials Science in Semiconductor Processing 16 (2013) 818–824

Contents lists available at SciVerse ScienceDirect

Materials Science in Semiconductor Processing

journal homepage: www.elsevier.com/locate/mssp

Photocatalytic and bactericidal activities of hydrothermally and sonochemically prepared Fe_2O_3–SnO_2 nanoparticles

C. Karunakaran*, S. SakthiRaadha, P. Gomathisankar

Department of Chemistry, Annamalai University, Annamalainagar 608002, India

ARTICLE INFO

Available online 9 March 2013

Keywords:
Nanocomposite
Magnetic separation
Visible light photocatalysis
Bactericide

ABSTRACT

Fe_2O_3–SnO_2 nanocomposites (NCs) were prepared by hydrothermal and sonochemical methods. Transmission electron micrographs confirmed that the composites comprise nanoparticles. Energy-dispersive X-ray analyses revealed compositions of 25 at.% Sn and 22 at.% Fe for hydrothermally prepared NC (HNC) and 4 at.% Sn and 56 at.% Fe for sonochemically prepared NC (SNC). X-Ray diffractograms revealed rutile SnO_2, γ-Fe_2O_3, and FeO(OH) as components of HNC, and rutile SnO_2, γ-Fe_2O_3, β-Fe_2O_3 and FeO(OH) of SNC. Both NCs absorb visible light and display red emission. The solid-state impedance spectrum for HNC is a half-semicircular arc and SNC exhibits a quasi-linear relationship between Z'' and Z'. Both NCs are ferromagnetic. The saturation magnetization of HNC is much less than that of the SNC, which in turn is far less than that of the γ-Fe_2O_3 precursor. Both NCs display visible light photocatalysis and HNC is a better photocatalyst than SNC. Furthermore, both NCs exhibit bactericidal activity.

1. Introduction

SnO_2 is the most studied semiconductor nanomaterial for sensor applications [1]. Its use as photoelectrodes in solar cells is well established [2]. Owing to its unique photoelectronic properties [3,4], non-toxicity, and chemical stability, it is also used as a photocatalyst [5–7]. The problem of nanopowder recovery after photocatalysis is a limitation for the adoption of this technology in industry. Magnetic separation of the photocatalyst is a possible solution [8] and Fe_2O_3–SnO_2 nanocomposites (NCs) are suitable for this purpose. Furthermore, SnO_2 is a wide-bandgap n-type semiconductor ($\sim$3.8 eV) and requires UV light of $<$330 nm for photocatalysis. Fe_2O_3 is a narrow-bandgap n-type semiconductor ($\sim$2.2 eV) and is photoactivated by visible light. However, the photogenerated hole in the valence band (VB) of Fe_2O_3 is less anodic than those in widely used photocatalysts such as TiO_2, ZnO, and SnO_2 and its oxidizing power is low [9]. By contrast, the hole in the VB of SnO_2 is more anodic (high oxidizing power) than in most widely used semiconductors [9]. Furthermore, the conduction band (CB) electron in photoexcited SnO_2 is less cathodic than that of Fe_2O_3 [9]. The difference in VB and CB edge potentials between SnO_2 and Fe_2O_3 leads to separation of photogenerated charge carriers across the heterojunction, which enhances photocatalytic activity. Fe^{3+}-doped SnO_2 nanoparticles have been prepared by sol–gel calcination and sol–gel hydrothermal methods and the absorption edge is red-shifted with increasing dopant content [10]. Fe-doped SnO_2 has also been prepared using an aqueous solution method [11]. However, it has been reported that Fe^{3+}-doping of SnO_2 suppresses sensing of methane [12]. By contrast, sol–gel-prepared Fe_2O_3-SnO_2 can sense gas concentrations of ethanol, carbon monoxide, and methane [13–15]. Fe_2O_3–SnO_2 obtained by mechanical alloying showed greater selectivity in sensing ethanol gas compared to carbon monoxide and hydrogen [16]. Fe_2O_3–SnO_2 prepared by a wet chemical method was used to

* Corresponding author. Tel.: +91 9443481590; fax: +91 4144238145.
E-mail address: karunakaranc@rediffmail.com (C. Karunakaran).

1369-8001/$ - see front matter © 2013 Elsevier Ltd. All rights reserved.
http://dx.doi.org/10.1016/j.mssp.2012.12.030

sense hydrogen sulfide [17]. Liquefied petroleum gas can also be sensed by SnO_2–Fe_2O_3 films [18]. Hydrothermally prepared 0.1 SnO_2–0.9 α-Fe_2O_3 was used to sense methane and carbon monoxide [19], where Fe^{3+} was substituted by Sn^{4+}. Fe_2O_3–SnO_2 obtained by a co-precipitation method showed efficient electron–hole separation [20]. SnO_2–Fe_2O_3 can also be obtained by chemical precipitation [21,22]. SnO_2–α-Fe_2O_3 composite nanowire arrays have been obtained by electrophoretic deposition [23]. α-Fe_2O_3–SnO_2 NC showed lattice mismatch at the interface [24]. Sol–gel-prepared α-F_2O_3–SnO_2 film showed greater photoelectrochemical properties [25]. SnO_2–α-Fe_2O_3 heterostructures fabricated by chemical vapor deposition showed enhanced photocatalytic activity due to improved electron–hole separation [26]. Fe_2O_3–SnO_2 NC obtained by co-precipitation exhibited visible light photocatalysis [27]. Branched SnO_2–α-Fe_2O_3 semiconductor nanoheterostructures were recently synthesized hydrothermally. The heterostructures showed excellent visible light and UV photocatalytic abilities that were remarkably superior to those of the α-Fe_2O_3 precursor, mainly owing to effective electron–hole separation at the SnO_2–α-Fe_2O_3 interface [28]. Sonochemical and hydrothermal methods are solution synthesis techniques. In the latter, chemical transformation occurs in supercritical aqueous solution. In the former, the chemical effects of ultrasound arise due to acoustic cavitation, which involves the formation, growth, and implosive collapse of bubbles in aqueous solution. Localized hotspots are produced through adiabatic compression. The transient temperature and pressure associated with these hotspots are as high as 5000 K and 1800 atm., respectively, and the cooling rate is as great as 10^{10} K s^{-1} [29]. These extreme conditions lead to chemical reaction. Although there are reports on the synthesis of Fe_2O_3–SnO_2 NCs using the methods mentioned above, there are no reports on the synthesis of Fe_2O_3–SnO_2 NC by sonochemical and hydrothermal solution methods using the same precursor and reagents for comparison of their photocatalytic and bactericidal activities. Our results show that for Fe_2O_3–SnO_2, hydrothermally synthesized NC (HNC) exhibit greater photocatalytic and antibacterial activities than sonochemically prepared NC (SNC).

2. Experimental

2.1. Materials

Stannous chloride (Qualigens), hydrogen peroxide (SD Fine), sodium hydroxide (SD Fine), poly(ethylene glycol) (PEG, 20 000; Himedia), hexamine (Himedia) and rhodamine B (SD Fine) of LR grade were used as received. Phenol (AR, SD Fine) was distilled before use. Fe_2O_3 nanopowder (Sigma Aldrich) was used as received. Distilled ethanol and deionized distilled water were used for the experiments.

2.2. Hydrothermal and sonochemical preparation

To an ethanolic solution of PEG (2 g in 10 ml) was added 0.37 g of Fe_2O_3 nanopowder under constant stirring (for HNC) or sonication (for SNC; Toshcon SW2 ultrasonic bath, 100 W at 37 ± 3 kHz) to obtain a suspension. Then 20 ml of a 1:1 aqueous ethanolic alkaline (1.8 M NaOH) solution of H_2O_2 (7.5% v/v) was added under stirring (for HNC) or sonication (for SNC). To the resulting dispersion, 30 ml of an ethanolic solution containing 1.4 g $SnCl_2$ and 1.0 g hexamine was added dropwise with stirring (for HNC) or sonication (for SNC). The mixture was either sonicated for 30 min to obtain a brown solid or transferred to a Teflon-lined stainless steel autoclave for hydrothermal treatment. The autoclave was sealed, kept at 180 °C for 12 h and allowed to cool to room temperature naturally to obtain a brown solid. In both cases the solid was separated, washed several times with water and absolute ethanol, and finally dried at 120 °C for 4 h. The product was calcinated at 500 °C for 2 h in a muffle furnace fitted with a PID temperature controller. The heating rate was 10 °C min^{-1}. A schematic diagram of the synthesis methods is shown in Fig. 1. Pristine SnO_2 nanocrystals were synthesized hydrothermally and sonochemically using the same procedure but without Fe_2O_3.

2.3. Characterization techniques

A JOEL JSM 5610 scanning electron microscope (SEM) equipped with BE detector was used to examine the sample morphology. Samples were placed on an adhesive carbon slice supported on copper stubs and coated with 10-nm-thick gold using a JOEL JFC-1600 auto fine-coater prior to measurement. Transmission electron microscopic (TEM) analysis was carried out using a JEOL 100CX II

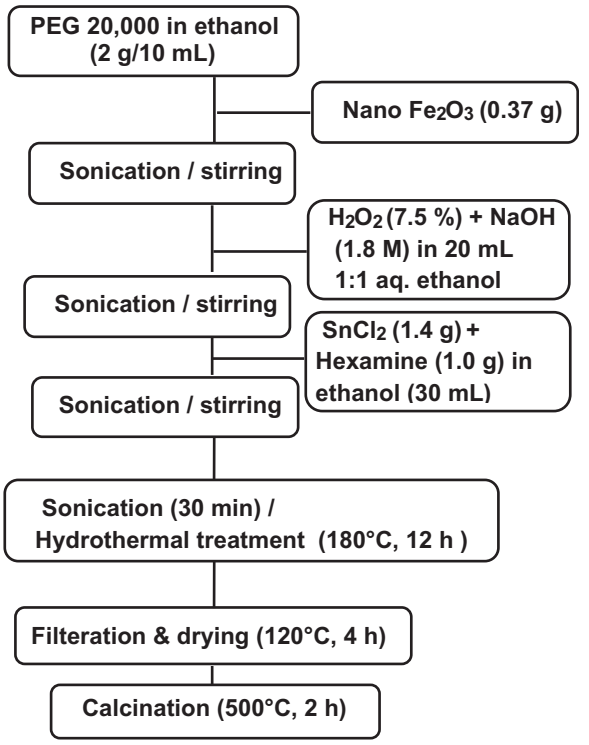

Fig. 1. Scheme for hydrothermal (H) and sonochemical (S) preparation of Fe_2O_3–SnO_2.